Desalination and Water Treatment
www.deswater.com

doi: 10.5004/dwt.2023.29782

303 (2023) 224–235
August

Polymer microgel-based gold nanocomposites for reductive degradation of azo dyes

Mehrab Khan[a], Sadia Iqbal[a], Sara Musaddiq[a,*], Fauzia Iqbal[b], Javeria Kanwal[a], Sajjad Ahmad[c]

[a]*Department of Chemistry, Kutchery Campus, The Women University Multan, Multan 60000, Pakistan, emails: mehrab0702@gmail.com (M. Khan), sadia.iqbalshahid@gmail.com (S. Iqbal), drsara.chem@wum.edu.pk (S. Musaddiq), javeriakanwal13@gmail.com (J. Kanwal)*
[b]*Department of Physics, University of The Punjab, Lahore, Pakistan, email: fauziaiqbal11@gmail.com*
[c]*Pakistan Council of Research in Water Resources, Ministry of Science and Technology, Pakistan, email: chsajjadahmad@hotmail.com*

Received 24 February 2023; Accepted 13 July 2023

ABSTRACT

Stimuli responsive polymer microgels have gained attention due to their envisioned applications. The aim of this study is to organize Au-based poly(N-isopropylmethacrylamide-co-acrylamide) [Au-p-(NIPMAM-co-AAm)] microgels and to analyse their degradation potential. Microgels were analyzed via UV-Visible (ultraviolet–visible) spectroscopy, X-ray diffraction and Fourier-transform infrared spectroscopy. Reductive degradation of Congo red (CR) was done to evaluate the catalytic activity of Au-based p-(NIPMAM-co-AAm) microgels that converts CR into less toxic products, that is, sodium 4-amino-1-naphthalene sulfate and biphenyl. Kinetic study of reaction reveals first order reaction and by altering the concentration of Congo red (CR) dye from 0.02 to 0.095 mM, the change in apparent rate constant (k_{app}) was noted from 0.0027 to 0.1235 min^{-1}. Whereas the change in value of rate constant (k_{app}) was observed from 0.0716 to 0.2931 min^{-1} as catalytic dose was changed from 0.06 to 0.1 mL (60–100 μL) at certain temperature. Reduction efficiency of recycled Au-based p-(NIPMAM-co-AAm) was also deliberated and not any remarkable reduction was observed in the percentage catalytic efficiency of nanocomposite until four cycles.

Keywords: Catalytic reduction; Kinetics; Composite microgels; Congo red; Au nanoparticles

1. Introduction

Environmental pollution is one of the most important worldwide problems as rapid industrialization is causing discharge of many environmental pollutants into the environment [1]. A lot of industrial processes like leathering, clothing, pulping and paper, pharmaceuticals, tanneries, cosmetics and electroplating are using many chemicals including organic azo dyes. Because of their rapid synthesis and large number of implementations, organic dye stuffs have set off as an essential fraction of industrial wastewater [2]. Light entering in water, absorbed by these organic dyes destroy the balance of the aquatic system [3]. Dyes generally contain elements like nitrogen, sulfur or chlorine. The products attained after the oxidation of these type of harmful moieties could be more dangerous than the original molecule [4]. So, degradation of such hazardous chemicals from the polluted or dissipated water is a demanded topic of ongoing research [5].

For the dye removal from wastewater, many physical [6], chemical [7] and biological [8] methods have been widely reported. Furthermore, many new chemical methods are used for the degradation and/or removal of these organic pollutant [6] such as membrane filtration, photocatalytic

* Corresponding author.

degradation [9], chemical oxidation [10], coagulation [11], radiolysis [12], flocculation [13] and adsorption [14]. Now-a-days, the use of nanoparticles increased enormously because of their wide range application in many technological areas such as optics, biotechnology, electronics and chemical catalysis [15]. However, metal nanoparticles agglomerate themselves very speedily to lower their surface to volume ratio thus reducing catalytic efficiency of these metal nanoparticles. Different types of stabilizing moieties like micelles, block copolymers, dendrimers, polysaccharides and microgels [16] have been used to stop aggregation of these metal nanoparticles. Among these, microgels have gained much importance due to many factors like easy synthesis, simple functionalization, versatile dimensions, consistent size arrangement and their immediate feedback to external stimulant such as pH, light and temperature [5]. Metal nanocomposites like gold, platinum, copper, iron, palladium and silver have been assembled and reported their applications as a catalyst. The prepared material was not only cost effective but more efficient also. Microgel-based systems have a huge span of applications just because of their easy synthesis and their quick response to external stimuli [17]. Microgels could be recycled very efficiently from the reaction mixture by using centrifugation method and hence can be reused.

Due to the interconnected polymer network, these micro gels can stand stable for everlasting, and this polymer lattice cannot be reduced even by repeated agitation and centrifugation [13]. Other low-cost materials like Zn [18] and Cd-based nanoparticles form oxides very rapidly and loss their stability while Au-based nanocomposites resist oxidation and even stable for many months. Microgels have colloidal dimensions, that is, 1 nm–1 μm, consequences from a polymerization reaction and have a capability to answer to external factors [19]. In current years, many NIPAM-based microgels could be utilized for the degradation of synthetic dyes from the polluted water [20]. Here we have reported the synthesis of polymer micro gels fabricated with gold nanoparticles. The fabrication of Au nanocomposite having temperature-responsive polymeric microgels are termed as hybrid microgels and these hybrid microgels has been used in various applications such as tunable catalysis [21], sensing [22] and drug delivery [23] and for the breakdown of organic contaminants [24]. So, preparation of stable and cheap catalyst for the degradation of toxic compounds is desirable. In this aspect, polymer microgel-based metal nanocomposite have attained too importance as a catalyst applied for the degradation of organic pollutants [25].

Here, we have reported the most efficient method used for the breakdown of hazardous dye (Congo red) by using sodium borohydride ($NaBH_4$) and hybrid microgels (polymer microgels-based gold NPs) as catalyst [26]. We can treat industrial wastewater by using hybrid microgel as a catalyst. Based on superb catalytic activity of Au-p(NIPMAM) for successful degradation of several dyes individually, the system can be used to perform degradation of dyes present in industrial wastewater collected from local textile industry which is desirable as most of textile industrial wastewater is discharged into environment without any conventional treatment which is causing significant health problems.

2. Experimental set-up

2.1. Materials

N-isopropylmethacrylamide (NIPMAM) (96%), acrylamide (AAm) (98%), ammonium persulfate (98%, APS), N,N′-methylenebisacrylamide (99%) (BIS), sodium dodecyl sulfate (SDS), sodium borohydride (99%) ($NaBH_4$), chloroauric acid gold(III) chloride hydrate [$HauCl_4 + 3H_2O$], were purchased from Sigma-Aldrich (Germany). All experiments together with synthesis and catalytic applications were done in deionized H_2O. A porous membrane tube for dialysis was owned having molecular weight value of approximately 12,000–14,000 g/mol utilized to purify microgels and hybrid micro gels was purchased from Sigma-Aldrich.

2.2. Fabrication of p-(NIPMAM-co-AAm) microgels

Poly-(NIPMAM-co-AAm) microgels molecules with little bit moderation were prepared by free radical co-precipitation polymerization method. In three necked round bottom flask, 95 mL distilled water was poured in flask in which 1.5376 g (0.01209 mol) of N-isopropylmethacrylamide as main monomer and 0.03696 g (0.00052 mol) of acrylamide as comonomer, 0.060 g (0.00039 mol) of BIS as a cross-linker, 0.06 g of SDS as surfactant were also poured and stirred about 45 min via heating. When the temperature approached up to 70°C then 5 mL of APS solution (0.05 M) as an initiator was poured into reaction mixture. Reaction was further carried out for 4–5 h at around 70°C. Total number of moles of reaction mixture was kept 0.013. All the reaction was carried out in inert atmosphere provided by nitrogen supply through special type of condenser known as Friedrich Condenser. Poly-(N-isopropylmethacrylamide-co-acrylamide) microgel had been prepared then it is passed through molecular porous dialyzing membrane against distilled water via stirring for 72 h at room temperature.

2.3. Fabrication of Au-based p-(NIPMAM-co-AAm) hybrid microgels

The fabrication of gold nanoparticles was carried out within polymer microgels. More precisely, the microgel dispersion (18 mL) and distilled water (6 mL) were mixed and stirred under N_2 purging at room temperature for 30 min. [$HAuCl_4 + 3H_2O$] aqueous solution (3 mL, 2 mM) was added into the dispersion and stirring was carried out for 1 h at room temperature. Later on, freshly prepared solution of $NaBH_4$ (3 mL, 4 mM) was added drop wise into the reaction mixture and further stirring was continued for 1.5 h. The color of micro gel suspension was turned from colorless to dark brown hybrid micro gel dispersion was dialyzed for 1 h at room temperature with frequent exchange of distilled water to remove unreacted species.

A hybrid microgel was prepared by *in-situ* reduction of gold ions (Au^+) inside the network of p-(NIPMAM-co-AAm) microgels [17]. For this purpose, 18 mL of prepared microgel and 6 mL of distilled water was poured into three necked round bottom flask and continuous stirring was held via purging with N_2 cylinder. After 30 min later 3 mL of 0.002 molar solution of [$HAuCl_4 + 3H_2O$] was injected into the reaction vessel and allowed to stir it for 1 h at room

temperature After that 0.0035 g of sodium borohydride was dissolved in 3 mL of distilled water and was immediately injected into the reaction vessel dropwise. Simultaneously, color of reaction mixture becomes greenish brown which depicts the generation of Au nanocomposites from Au ions as shown in Fig. 1. Stirring was carried out for more 1 h further. Au-Poly-(N-isopropylmethacrylamide-co-acrylamide) microgel had been prepared and dialyzed it against distilled water through dialyzing membrane for 2 h.

2.4. Characterization

The particle size and arrangement of both pure and hybrid microgel were acquired by UV-Vis spectrum, Fourier-transform infrared spectroscopy (FTIR), transmission electron microscopy and scanning electron microscopy (SEM). The specimen for SEM were fabricated with vapors of platinum metal before characterization. Dynamic light scattering technique was utilized to check the temperature sensitive nature of microgels as well as their hydrodynamic diameters. X-ray energy dispersive technique was used for studying the configuration of pure and hybrid microgels. For energy-dispersive X-ray analysis measurement, the samples are not laminated with gold or Pt vapors. UV-Vis spectroscopy was done with a double beam UV spectrophotometer equipped with a temperature controller with a wavelength range of 200–700 nm.

2.5. Catalytic degradation of Congo red

First, different concentration solutions of Congo red (CR) such as 0.095, 0.08, 0.065, 0.05, 0.035, and 0.02 mM were prepared. Quartz sample cell having fixed path length of 2.5 cm was used in this procedure and in this cell 1.8 mL of CR solution with different concentration was poured one by one. To this, 0.5 mL (500 μL) of $NaBH_4$ and 0.035 mL (35 μL) [Au-p-(NIPMAM-co-AAm)] catalyst as constant constituents were poured into cells. UV spectra were recorded after every 2 min until the whole solution turns colorless. Similar procedure was replicated for 0.095 mM CR solution by varying amount of hybrid microgel [Au-poly-(NIPMAM-co-AAm)] (catalyst) as 0.06 mL (60 μL), 0.07 mL (70 μL), 0.08 mL (80 μL), 0.09 mL (90 μL), 0.1 mL (100 μL), respectively. This catalytic process was repeated by using different concentration solutions of dye and spectra were recorded every 2 min.

3. Result and discussion

3.1. Mechanism for fabrication of p-(NIPMAM-co-AAm)

Free radical co-precipitation polymerization mechanism was involved in the preparation of p-(NIPMAM-co-AAm) microgels in the aqueous medium. The monomer (NIPMAM) and the cross linker (BIS) are water soluble. Microgel synthesis was started when the temperature raised upto 70°C because the initiator molecules are decomposed at this particular temperature and as a result sulfate free radicals (SO_4^{-2}) are produced. Insoluble polymeric chains are synthesized when the unpaired electron present on the sulfate radical starts polymerization by the reaction with monomer. Free radical and negative charge on the opposite end are present on these insoluble polymeric chains. When the reaction temperature raised to 70°C, these insoluble polymeric chains collapsed with each other and make a globular formation that acts as pioneer particles for formation of microgel. To gain stability, these pioneer particles agglomerate with the other parent particles present in the reaction mixture to form colloidally fixed microgels

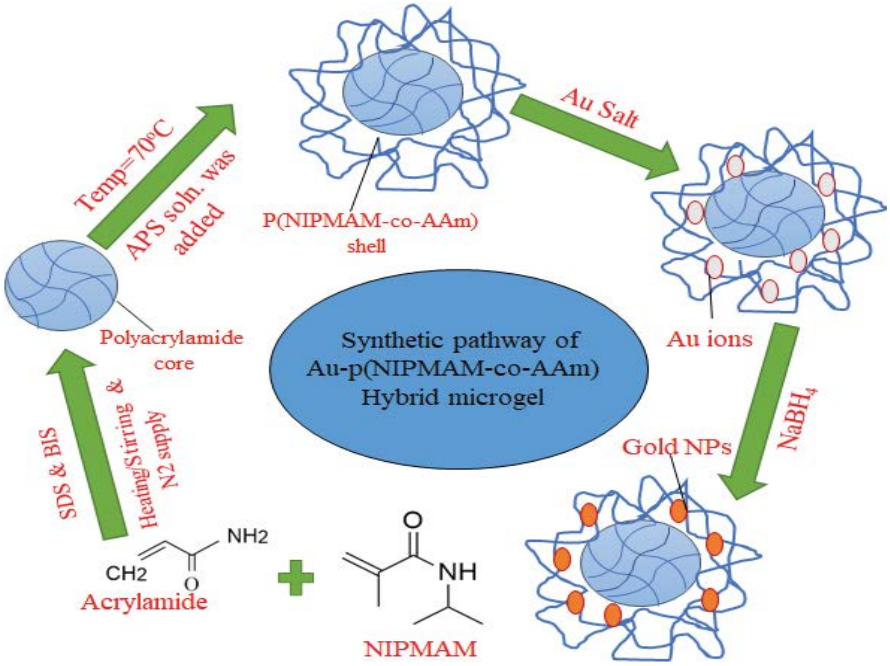

Fig. 1. Synthetic representation of Au-p(NIPMAM-co-AAm) hybrid microgel.

lattice. Negative moiety that is produced by initiator is also contributed to generate coalescence between small parent's particles and stabilize that also at higher temperature. To increase this electrostatic stability, cross linker BIS also take part in reaction and involved in the cross linking of microgel and due to this different pore sized particles are formed. Reaction mixture becomes translucent upon the addition of APS that shows the change in refractive index value of microgel particles and permits indication about start of polymerization reaction. Proper stability as well as monodispersity among microgel particles gained by the addition of surfactant SDS. When the polymerization process is completed, the whole mixture is cooled at room temperature. As a result, swollen state microgel particles are generated.

3.2. Mechanism for fabrication of Au-based p-(NIPMAM-co-AAm)

Diluted microgel dispersion was treated with chloroauric acid gold(III) chloride hydrate [$HAuCl_4 + 3H_2O$] salt for the fabrication of Au NP's into the p-(NIPMAM-co-AAm) microgel network. Solution of chloroauric acid gold(III) chloride hydrate acts as a precursor of Au NP's. Swelling micro gel particles are contributed for maximum fabrication of Au^+ ions. Addition of reducing agent that is sodium borohydride into the reaction media is responsible for the reduction of gold atoms. Sodium borohydride decomposes into Na^+ ions and borohydride ions when it is added into the reaction mixture. Due to the presence of lone pair, the borohydride ion attracts towards Au^+ ions present in pores of microgel and changed into gold atoms. These Au atoms are merged to produce gold nanoparticles. Colour of micro gel dispersion was altered from milky appearance to yellowish brown as a result of the insertion of $NaBH_4$ that shows eminent reduction of Au ions into gold atoms and fabrication of Au NP's inside structure of microgel. Due to extensive cross-linking present in polymeric chains, the microgel particles exceed up to nano range leads to formation of nanoparticles of gold [27].

3.3. FTIR analysis for both p-(NIPMAM-co-AAm) and Au-based p-(NIPMAM-co-AAm) microgel

FTIR technique was utilized to evaluate the functional entities existing in the polymeric network of pure microgel and hybrid microgel. FTIR analysis also gives information about the interaction of these functionalities with metal nanoparticles. FTIR spectrum of both poly-(NIPMAM-co-AAm) and Au-p-(NIPMAM-co-AAm) pure and hybrid microgel are given in Figs. 2 and 3, respectively.

Polymeric microgel possess all functionalities as present in monomers and it is confirmed by FTIR analysis. The broad and intense peak is observed at 3,349 cm^{-1} shows the presence of N–H stretching signals of p-(NIPMAM-co-AAm) pure microgel while this vibration is observed at 3,366 cm^{-1} in case of Au-p-(NIPMAM-co-AAm) hybrid microgel. The N–H stretching signal observed in poly-(NIPMAM-co-AAm) microgel network indicates the existence of hydrogen bonding with H_2O molecules coupled to the polymeric microgel [24]. This band becomes vaster in case of Au-p-(NIPMAM-co-AAm) hybrid microgel. It occurs because the water molecules are lost adjacent within the polymeric microgel upon fabrication of gold nanoparticles. Absorption peak observed at 2,970 and 2,971 cm^{-1} in both the pure microgel and also in hybrid microgel accordingly shows the anti-symmetric C–H stretching vibrations. Carbonyl group present in the pure microgel shows their characteristic peak at 1,625 cm^{-1}. In case of Au-p-(NIPMAM-co-) hybrid microgel, absorption band observed at 1,626 cm^{-1} indicates the donor–acceptor interactions of carbonyl group with gold nanoparticles commenced in their surroundings. Broad peak observed at 1,509 cm^{-1} in polymeric microgel shows the destruction of N–H bond. No any absorption peak in both spectra of pure microgel and hybrid microgel shows the presence of vinyl group. It confirms the transformation of C=C into C–C due to polymerization [28]. Two broad peaks present at 1,386 and 1,366 cm^{-1} in these two pure and hybrid microgel attributes the methyl group bending signals and stretching signals for C–N accordingly. Due to the interconnection of metal nanocomposite with

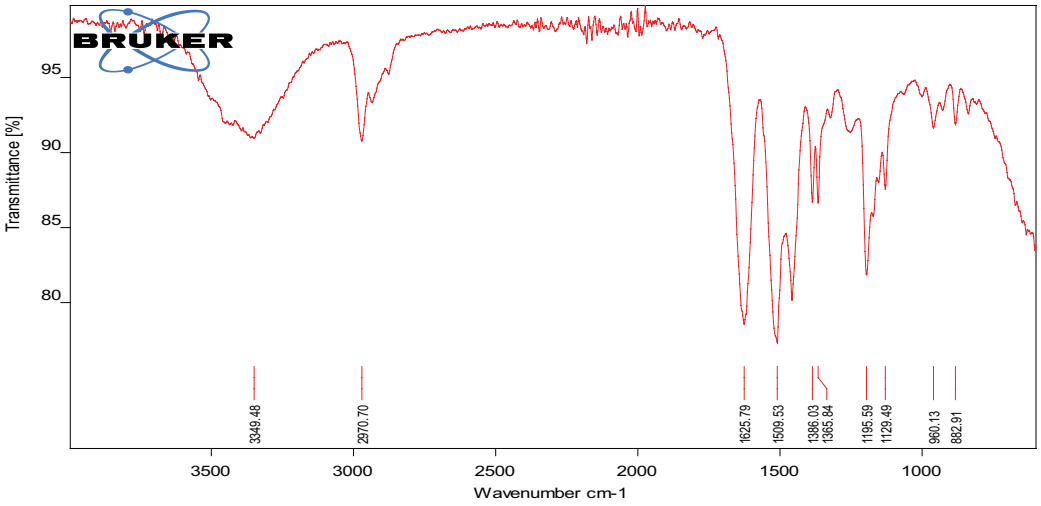

Fig. 2. Fourier-transform infrared spectra of p-(NIPMAM-co-AAm) microgel.

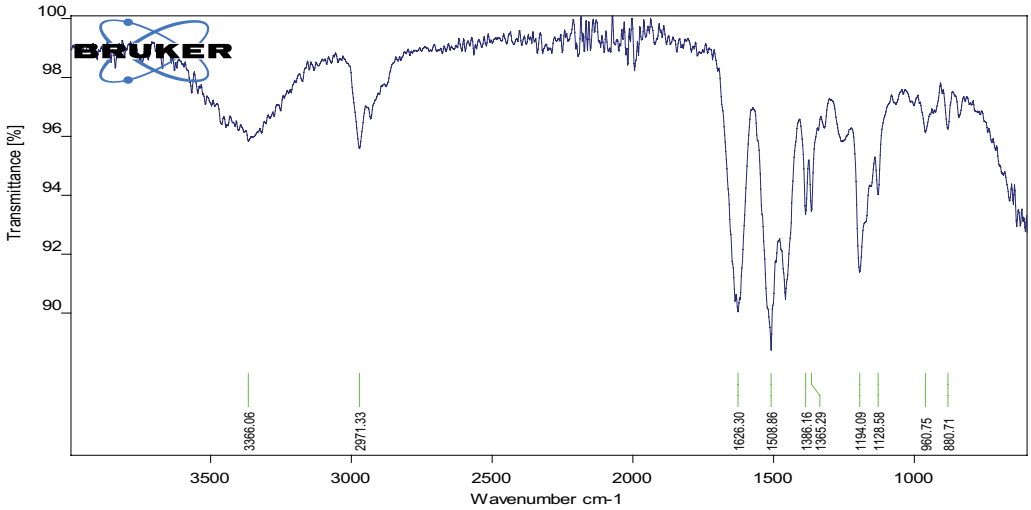

Fig. 3. Fourier-transform infrared spectra of Au-p-(NIPMAM-co-AAm) hybrid microgel.

the functional groups existing in the microgel lattice, little change in the orientation and intensity of several absorption bands in FTIR spectrum of both microgel and hybrid microgel was observed. Farooqi et al. also evaluated the numerous functional entities of p-(NIPMAM-co-MAA) pure and hybrid microgel through FTIR analysis and their results shows correspondence with our FTIR spectra [1]. Some absorption bands are also observed in far infrared region of FTIR spectrum due to the linkage of metal nanocomposite with the various functional groups located in polymeric microgel lattice.

3.4. UV-Vis analysis of p-(NIPMAM-co-AAm) and Au-based p-(NIPMAM-co-AAm)

Double beam UV-Visible spectrophotometer was operated for the analysis of pure and hybrid microgel. Fig. 4 shows the UV-Visible spectrum of watery dispersion of pure and hybrid microgel. In UV-Visible spectrum of p-(NIPMAM-co-AAm) microgel dispersion, NIPMAM, acrylamide and BIS units are transparent towards UV-Visible radiation and hence not exhibit any particular peak in UV-Visible range [27]. While Au-p-(N-isopropylmethacrylamide-co-acrylamide) hybrid microgel shows a characteristic peak at 520 nm that exhibits the phenomenon of surface plasmon resonance (SPR) of gold nanoparticles because of their interaction with electromagnetic radiations. Peak observed at 520 nm gives a clear sign of gold nanoparticles having small size distribution [29]. Kinetic study of catalytic degradation of Congo red was also calculated by the use of UV-Visible spectroscopy.

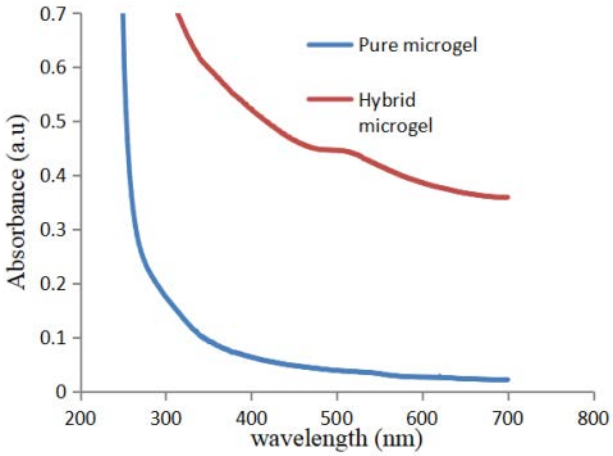

Fig. 4. UV-Vis spectra of poly-(NIPMAM-co-AAm) microgel and Au-poly-(NIPMAM-co-AAm) hybrid microgel.

3.5. X-ray diffraction analysis of Au-based p-(NIPMAM-co-AAm) hybrid microgel

X-ray diffraction (XRD) pattern for the Au-poly-(NIPMAM-co-AAm) microgel as shown in Fig. 5. The various peaks obtained in XRD pattern give information about the crystalline nature of gold nanoparticles inside the microgel network. Characteristic peaks of the gold were not observed if the size of crystal was very small or crystalline arrangement was not fully formed. The various peaks for gold nanoparticles secured at 2θ angles of 77.6°, 64.5°, 38.1°, and 44.3° were related to the crystalline planes (111), (200), (220) and (311), respectively of gold nanoparticles [26]. In XRD pattern of hybrid microgel, intense peak observed at 38.1° shows that the crystalline gold nanoparticles entrapped inside the microgel network. The average dimension of the gold nanocomposite crystalline domains was studied by Debye–Scherrer calculations from the XRD data.

3.6. SEM analysis of poly-(NIPMAM-co-AAm) and Au-based poly-(NIPMAM-co-AAm)

SEM analysis was performed to find out the surface morphologies (size, shape and dispersion) of pure microgel and hybrid microgel particles. The p-(NIPMAM-co-AAm) microgel and gold nanocomposites are round in configuration with diameter less than 20 nm [26].

4. Catalytic efficiency of Au-poly-(NIPMAM-co-AAm) hybrid microgel for degradation of Congo red

Anionic azo dyes salt including Congo red (CR) is an and it is majorly cast off in plastic, clothing, food and pulp industries. It has many harmful and toxic effects [7]. It is carcinogenic dye also called as metabolize benzidine (having benzidine group). Its aromatic structure provides it thermal, physico-chemical and optical stability [30]. As it is widely used in industries so it embellishes an utmost source of water fouling and have many harmful consequences for life on earth and also for life beneath water. Degradation of CR in aqueous media in the presence of $NaBH_4$ as degrading agent with no one catalyst is not kinetically suitable reaction. Catalyst helps to transfer electrons from borohydride ion to Congo red molecules. Metal nanoparticles are considered to be the best to do this [7]. Fig. 6 descripts the no change in colour of Congo red solution without using hybrid microgels.

The aqueous solution of Congo red shows two characteristic signals in UV-Vis region. One peak is observed at 490 nm due to allowed π–π* transitions and second peak is observed at 340 nm due to forbidden n–π* transitions associated to all azo compounds. Intensity of the absorption peaks is not affected by adding only $NaBH_4$ as degrading agent in the aqueous solution. Reduction of peak intensity has observed when little amount of Au-p-(NIPMAM-co-AAm) hybrid microgel is introduced as catalyst into the mixture. Dye was degraded not adsorbed because after degradation two new peaks are clearly observed that shows that the much toxic CR dye was converted into less hazardous fragments. The swap in absorbance of peak observed at 492 nm was studied to record the progress of catalytic degradation of CR dye that gently dropped with time. One peak is observed at 288 nm due to n–δ* transitions and the second one is observed at 249 nm due to δ–δ* transitions. These peaks give a clear conformation about the reduction of azo (–N=N–) into –NH–NH– [31]. Degradation products of toxic CR dye are sodium 4-amino-1-naphthalenesulfonate and biphenyl. The reaction was done by using two different operating conditions. Firstly, procedure was completed by differing concentration of dye from 0.02 to 0.095 mM, respectively and by using hybrid microgel [Au-p-(NIPMAM-co-AAm)] and 0.05 mL/50 μL $NaBH_4$ as constant

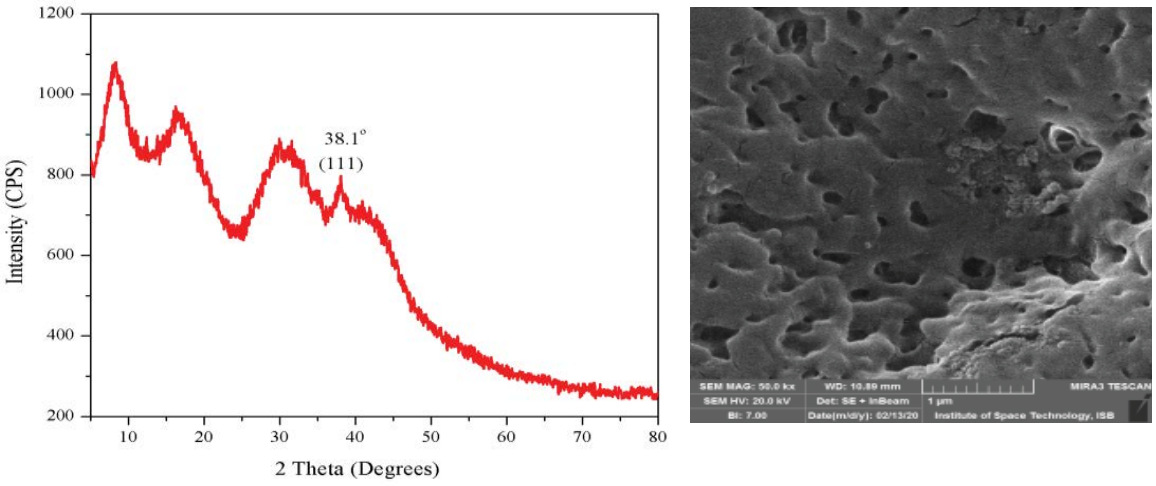

Fig. 5. (a) X-ray diffraction pattern for p-(NIPMAM-co-AAm) microgel and (b) scanning electron microscopy image of dispersion of P(NMA) hybrid microgels at pH 7.

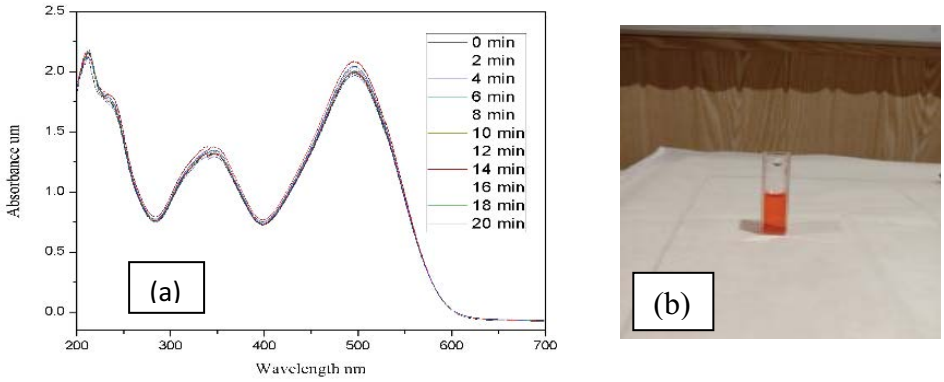

Fig. 6. (a) UV-Visible spectrum showing the catalytic degradation of Congo red without using hybrid microgel and (b) no change in color of Congo red without using catalyst.

for all CR solutions. Different graphs are obtained through UV-Visible spectrophotometer, and all are represented in Fig. 10. Secondly, reaction was performed by keeping concentration of dye and 0.05 mL $NaBH_4$ as constant factors and the amount of catalyst varied from 0.01 to 0.06 mL, respectively and the graphs of these reactions are shown in Fig. 13. Results obtained from these two operating conditions shows that degradation of the Congo red degradation is not possible by using only $NaBH_4$ without using catalyst. Disappearance of the color of dye and decrease in intensity of peaks upon addition of catalyst gives a clear indication that degradation of dye occurred. Catalyst was taken in very little quantity as compared to the amount of reducing agent so that peak intensity of CR is not effected by the plasmonic band of gold. To meet pseudo-first-order equation, dye was taken in a very little amount compared to amount of $NaBH_4$. Pseudo-first-order equation was taken as:

$$\ln\frac{C_t}{C_o} = \ln\frac{A_t}{A_o} = -k_{app}t \quad (1)$$

where C_t/C_o represents the correspondence of concentration of ions that are present in dye solutions at any time to that present at the beginning of reaction. Concentration ratio can be restored by A_t/A_o, shows the correspondence of dye absorbance at a piece of time to the beginning of reaction. For first-order reaction, k_{app} is known as apparent rate constant. In the start of the reaction, the color of CR solution is red which gradually fades with time and colorless solution was obtained at the end indicates the completion of reaction. Fig. 7 depicts the mechanism for the catalytic reduction of Congo red molecules through sodium borohydride.

4.1. Effect on k_{app} by varying concentration of CR

Results obtained from first reaction condition show that different concentration of CR effects the degradation gradually. The time taken for completion of reaction elevates with the increase in dye concentration and this result was obtained by plotting $\ln(A_t/A_o)$ vs. time as shown in Fig. 8. Concentration of CR was varied from 0.02 to 0.095 mM and value of $NaBH_4$ and hybrid microgel was kept constant to find out the result of different CR concentration on the rate of k_{app}. At starting, the k_{app} value elevates with the increase of concentration of CR but after that value of k_{app} deceases with further rise in CR concentration and this was settled by plotting vs. dye concentration (mM) vs. k_{app} (min^{-1}) as shown in Fig. 9. The rate of k_{app} is maximum with 0.065 mM concentration of CR that shows 0.035 mL/35 μL is optimum value for the 0.065 mM concentration of CR that can be set as a reference value just to achieve maximum result. The fall in k_{app} value with the further elevation in dye concentration usually obeys Langmuir–Hinshelwood operation in which desorption of product back into solution from the surface of catalyst is involved. Fig. 10 shows the UV-Visible spectrum of different concentrations of CR dye.

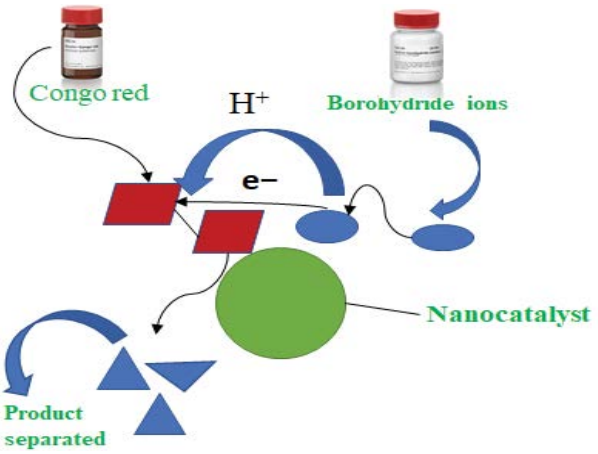

Fig. 7. Absorption of borohydride ions and Congo red on the surface of metal nanoparticles.

4.2. Effect on k_{app} by varying catalytic dose

In case of second reaction condition, the amount of catalyst increases from 0.01 to 0.06 mL and in this case, time taken for the achievement of process decreases. This was committed by the plot of time vs. $\ln(A_t/A_o)$ for varying the amount of catalyst as shown in Fig. 11. But the rate of

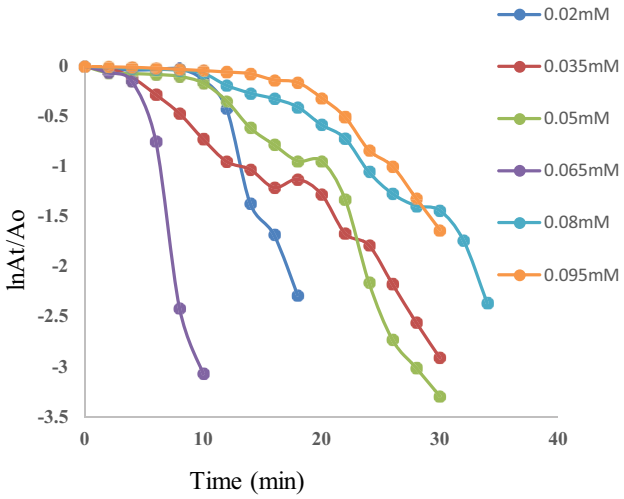

Fig. 8. Plot of $\ln(A_t/A_o)$ with respect to time for catalytic reduction of different concentration of Congo red dye with constant quantity of catalyst dose and $NaBH_4$.

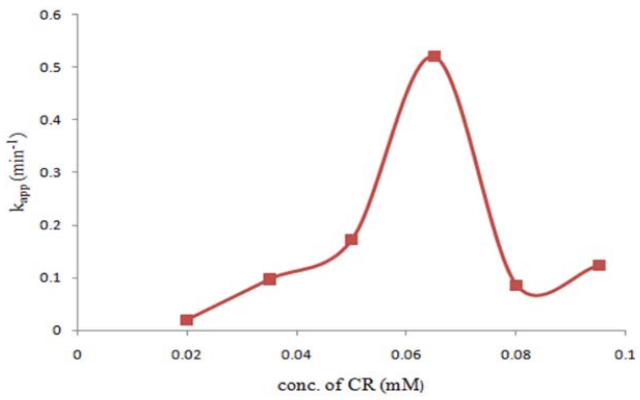

Fig. 9. Plot of k_{app} (min^{-1}) vs. concentration of Congo red (mM).

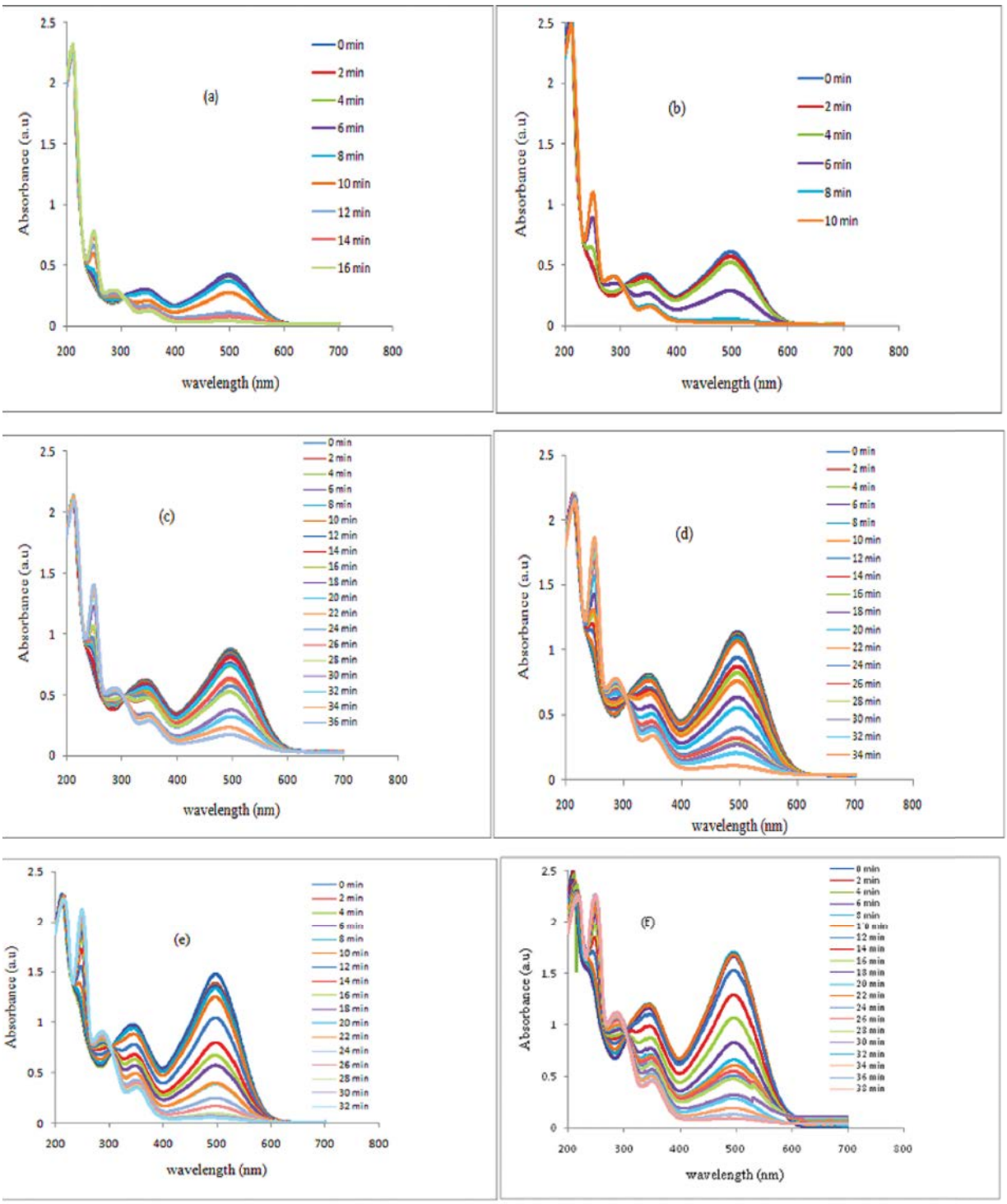

Fig. 10. UV-Visible spectra for degradation of Congo red solutions of different concentration having constant catalytic dose 0.035 mL/35 μL (a) for 0.02 mM Congo red, (b) for 0.035 mM Congo red, (c) for 0.05 mM Congo red, (d) for 0.065 mM Congo red, (e) for 0.08 mM Congo red and (f) for 0.095 mM.

constant shows elevation in this operating condition and it was established by graphing k_{app} (min^{-1}) vs. catalyst dose (mL) as indicated in Fig. 12. The value of k_{app} rises due to the elevation in number of NP's per unit volume by increase amount of catalyst. The percentage degradation of Congo red was found to be maximum where rate constant is high. Fig. 13 pointing out the UV-Visible spectrum for distinct concentrations of catalytic doses. For both the reaction conditions, Table 1 shows the value of apparent rate constant and their half-life. The time needed to decrease in the

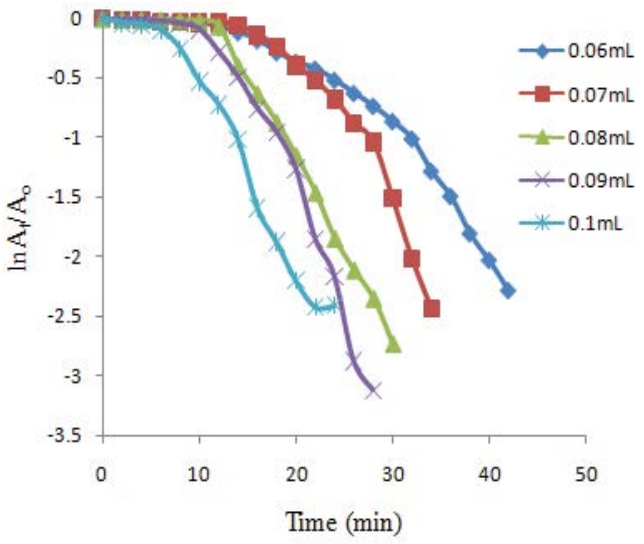

Fig. 11. Graph of $\ln(A_t/A_o)$ with respect to time for catalytic degradation of same concentration of Congo red dye and $NaBH_4$ with varying amount of catalyst dose.

concentration of the reacting substance by half is said to be its half-life. For pseudo-first-order mechanism, half-life can be deliberated by $t_{1/2} = 0.693/k$.

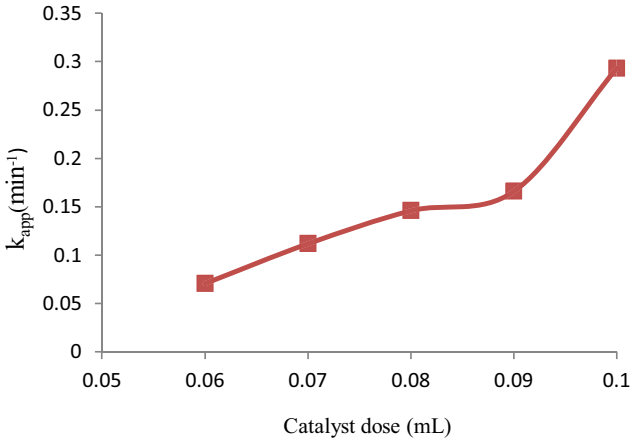

Fig. 12. Plot of k_{app} (min^{-1}) vs. catalyst dose (mL).

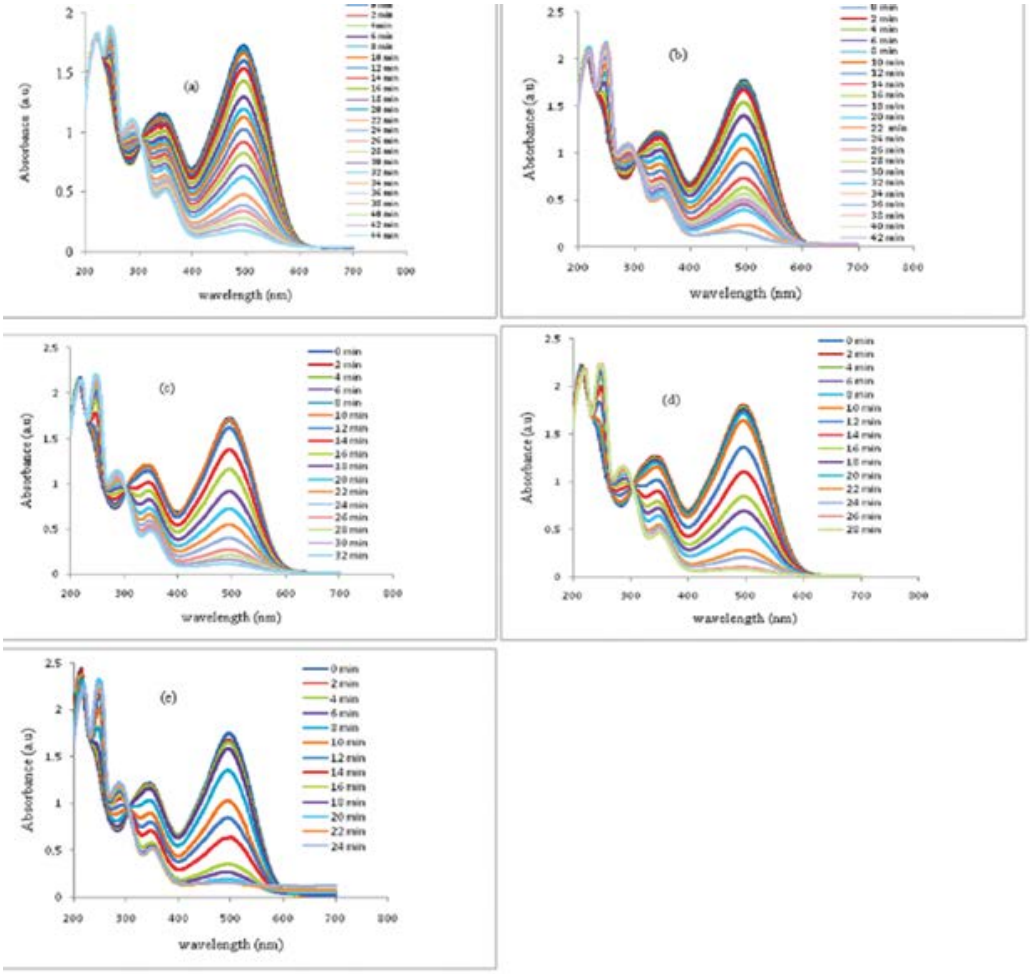

Fig. 13. UV-Visible spectra for degradation of Congo red solution having concentration of 0.095 mM by varying catalytic dose (a) 0.06 mL/60 μL, (b) 0.07 mL/70 μL, (c) 0.08 mL/80 μL, (d) 0.09 mL/90 μL and (e) 0.1 mL/100 μL.

Table 1
Apparent rate constant (k_{app}) and half-life of Congo red dye for both of operating conditions

Constant parameters	Variable parameters		Rate constant k_{app} (min^{-1})	Half-life (s)
Catalyst dose (0.035 mL/35 μL) + $NaBH_4$ (0.5 mL/500 μL)	Dye concentration	0.02 mM	0.0027	256.66
		0.035 mM	0.0972	7.12
		0.05 mM	0.1728	4.01
		0.065 mM	0.5207	1.33
		0.08 mM	0.0867	7.99
		0.095 mM	0.1235	5.61
Dye concentration (0.095 mM) + $NaBH_4$ (0.5 mL/500 μL)	Catalyst dose	0.06 mL	0.0716	9.67
		0.07 mL	0.1127	6.14
		0.08 mL	0.1462	4.74
		0.09 mL	0.1666	4.15
		0.1 mL	0.2931	2.36

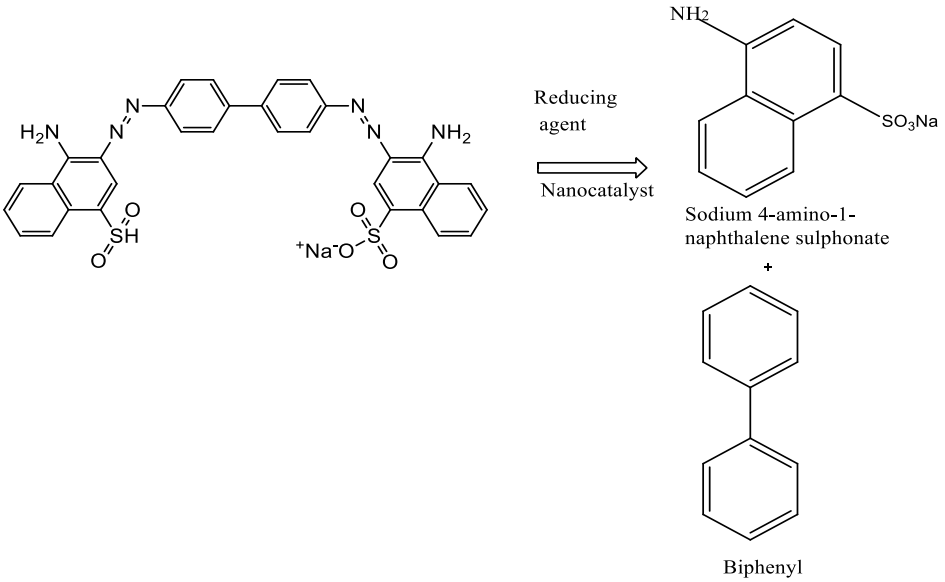

Fig. 14. Degradation products of Congo red.

5. Mechanism for the reduction of CR

As a result of decomposition of $NaBH_4$, Na^+ and BH_4^{-4} ions are produced in solution. Both the Congo red molecules and BH_4^{-4} ions are existing on the facet of gold nanocomposites. Borohydride ion acts as a source of hydrogen ion. Hydrogen is released when the borohydride ion present on metal nanoparticles surface transfer its electrons to metal nanoparticles. After gaining electrons, these metal nanoparticles now become active towards the diazo bond of Congo red molecules. CR entities are associated with metal nanocomposites through oxygen and sulfur atoms. As a result, the diazo bonds of Congo red molecules become weaken due to conjugation leading to breakage of azo bond. At the initial stage of reaction, the color of CR become fade and then it becomes colorless at the end of the reaction. This happens because of transformation of –N=N– connection into –NH–NH– bond and later the cracking of –NH–NH– bond. Product push off the surface of metal nanocomposite and escapes out at the end of the reaction. Biphenyl, Na salt of benzene sulphonic acid and N,N-dimethylaniline are the catalytic reduction end products of Congo red molecules [7]. as shown in Fig. 14.

To inspect the reproducibility of the synthesized catalyst, degradation of Congo red was used as a sample reaction. After execution of each degradation cycle, catalyst was isolated, washed, and dried to be utilized in the next cycle. The same conditions like Congo red (0.065 mM), sodium borohydride (15 mM) and Au-p(NIPMAM) (0.035 mL/35 μL) dispersion at 25°C, were sustained for each cycle to direct the percentage activity of the catalyst using following formula given in equation.

$$\%\text{Activity} = \frac{k_{app}(n)}{k_{app}(1)} \times 100 \quad (2)$$

Table 2
Gold nanoparticles stabilized in different systems have been reported as catalyst for catalytic degradation of Congo red

Stabilizing system	Catalyst used	Congo red	$NaBH_4$	k_{app} (min^{-1})	References
Dalspinin solution	100 μL	0.00001 mM	0.001 mM	0.0045	[32]
Salmalia malabarica gum	2,000 μL	1 mM	10 mM	0.236	[33]
Bacillus marisflavi	500 μL	1 mM	15 mM	0.2192	[34]
NIPMAM	100 μL	0.095 mM	5 mM	0.2931	This work

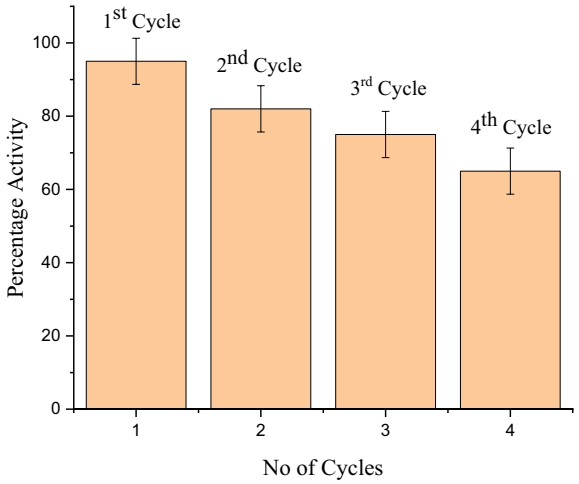

Fig. 15. Plot showing percentage activity after recycling of catalyst.

The structure of catalyst was stable as there was only a minute decrease in its catalytic efficiency which may be allocated to little fall in yield with each cycle due to loss of Au-p(NIPMAM) catalyst during its washing and drying. Fig. 15 depicts that the catalyst retains its activity for multiple cycles.

Summary of gold nanocomposites encapsulated on various supporting systems utilized for degradation of Congo red dye using $NaBH_4$ as reducing agent is shown in Table 2. The efficiency of catalytic system does not only influence on shape and size of nanoparticles encapsulated on various stabilizing systems but it is also simulated by stabilizing system.

The balancing of value of apparent rate constant for catalytic degradation of Congo red in the presence of Au-p(NIPMAM) hybrid polymeric system with previously reported in literature shows that our catalytic system is particularly operative for reductive degradation of Congo red in aqueous media.

7. Conclusion

By using monomer NIPMAM, comonomer AAm and cross-linker BIS, we have prepared p-(NIPMAM-co-AAm) microgel. By analyzing the FTIR spectrum of microgel, synthesis of microgel was fixed by the disappearance of band of C=C. Within the polymeric network of p-(NIPMAM-co-AAm) microgel, gold nanoparticles were formed and their fabrication within the polymeric network was settled by changing the milky appearance of microgel to brownish black. Then, synthesized Au-p-(NIPMAM-co-AAm) microgel was utilized as a catalyst to check the catalytic reduction of Congo red dye by using excess of $NaBH_4$ to fulfil the condition of pseudo-first-order reaction. Under two different operating conditions, we have calculated the rate constant (k_{app}) of these reactions. Initially, operating condition was fulfilled by using different concentration of dye and second by varying amount of catalyst. Then, apparent rate constant was calculated for pseudo-first-order mechanism. As a result of first operating condition, it was estimated that standard of k_{app} rises by elevating the concentration of Congo red by keeping other parameters constant and further rise in dye concentration cause fall in value of k_{app}. It was revealed from the kinetic measurements that the catalytic degradation of azo dyes obeys the Hinshelwood mechanism. But in second operating condition, it was seen that standard of k_{app} increases by rising the quantity of catalyst. By using high quantity of catalyst, the value of k_{app} is set out maximum.

References

[1] Z.H. Farooqi, K. Naseem, A. Ijaz, R. Begum, Engineering of silver nanoparticle fabricated poly(N-isopropylacrylamide-co-acrylic acid) microgels for rapid catalytic reduction of nitrobenzene, J. Pol. Eng., 36 (2016) 87–96.
[2] S.-M. Lam, J.-C. Sin, A.Z. Abdullah, A.R. Mohamed, Degradation of wastewaters containing organic dyes photocatalysed by zinc oxide: a review, Desal. Water Treat., 41 (2012) 131–169.
[3] K. Naseem, Z.H. Farooqi, R. Begum, M. Ghufran, M.Z.U. Rehman, J. Najeeb, A. Irfan, A.G. Al-Sehemi, Poly(N-isopropylmethacrylamide-acrylic acid) microgels as adsorbent for removal of toxic dyes from aqueous medium, J. Mol. Liq., 268 (2018) 229–238.
[4] B. Hameed, U. Akpan, K.P. Wee, Photocatalytic degradation of Acid Red 1 dye using ZnO catalyst in the presence and absence of silver, Desal. Water Treat., 27 (2011) 204–209.
[5] M. Ajmal, S. Demirci, M. Siddiq, N. Aktas, N. Sahiner, Simultaneous catalytic degradation/reduction of multiple organic compounds by modifiable p(methacrylic acid-*co*-acrylonitrile)–M (M: Cu, Co) microgel catalyst composites, New J. Chem., 40 (2016) 1485–1496.
[6] A. Akyol, M. Bayramoğlu, Photocatalytic degradation of Remazol Red F3B using ZnO catalyst, J. Hazard. Mater., 124 (2005) 241–246.
[7] J.-H. Sun, S.-P. Sun, G.-L. Wang, L.-P. Qiao, Degradation of azo dye Amido black 10B in aqueous solution by Fenton oxidation process, Dyes Pigm., 74 (2007) 647–652.
[8] N.P. Tantak, S. Chaudhari, Degradation of azo dyes by sequential Fenton's oxidation and aerobic biological treatment, J. Hazard. Mater., 136 (2006) 698–705.
[9] J.-L. Gong, B. Wang, G.-M. Zeng, C.-P. Yang, C.-G. Niu, Q.-Y. Niu, W.-J. Zho, Y. Liang, Removal of cationic dyes from aqueous solution using magnetic multi-wall carbon nanotube nanocomposite as adsorbent, J. Hazard. Mater., 164 (2009) 1517–1522.

[10] J.B. Fathima, A. Pugazhendhi, M. Oves, R. Venis, Synthesis of eco-friendly copper nanoparticles for augmentation of catalytic degradation of organic dyes, J. Mol. Liq., 260 (2018) 1–8.
[11] B. Xu, H. Zheng, H. Zhou, Y. Wang, K. Luo, C. Zhao, Y. Peng, X. Zheng, Adsorptive removal of anionic dyes by chitosan-based magnetic microspheres with pH-responsive properties, J. Mol. Liq., 256 (2018) 424–432.
[12] A.M. Aljeboree, A.N. Alshirifi, A.F. Alkaim, Kinetics and equilibrium study for the adsorption of textile dyes on coconut shell activated carbon, Arabian J. Chem., 10 (2017) S3381–S3393.
[13] K. Naseem, Z.H. Farooqi, R. Begum, A. Irfan, Removal of Congo red dye from aqueous medium by its catalytic reduction using sodium borohydride in the presence of various inorganic nano-catalysts: a review, J. Cleaner Prod., 187 (2018) 296–307.
[14] M.I. Din, K. Ijaz, K. Naseem, Biosorption potentials of acid modified *Saccharum bengalense* for removal of methyl violet from aqueous solutions, Chem. Ind. Chem. Eng. Q., 23 (2017) 399–409.
[15] D.J. Kim, S.M. Kang, B. Kong, W.J. Kim, H.J. Paik, H. Choi, I.S. Choi, Formation of thermoresponsive gold nanoparticle/PNIPAAM hybrids by surface-initiated, atom transfer radical polymerization in aqueous media, Macromol. Chem. Phys., 206 (2005) 1941–1946.
[16] S. Iqbal, S. Musaddiq, R. Begum, A. Irfan, Z. Ahmad, M. Azam, J. Nisar, Z.H. Farooqi, Recyclable polymer microgel stabilized rhodium nanoparticles for reductive degradation of para-nitrophenol, Z. Phys. Chem., 235 (2021) 1701–1719.
[17] M. Das, N. Sanson, D. Fava, E. Kumacheva, Microgels loaded with gold nanorods: photothermally triggered volume transitions under physiological conditions, Langmuir, 23 (2007) 196–201.
[18] N. Güy, M. Özacar, The influence of noble metals on photocatalytic activity of ZnO for Congo red degradation, Int. J. Hydrogen Energy, 41 (2016) 20100–20112.
[19] J.B. Thorne, G.J. Vine, M.J. Snowden, Microgel applications and commercial considerations, Colloid Polym. Sci., 289 (2011) 625–646.
[20] S. Iqbal, C. Zahoor, S. Musaddiq, M. Hussain, R. Begum, A. Irfan, M. Azam, Z.H. Farooqi, Silver nanoparticles stabilized in polymer hydrogels for catalytic degradation of azo dyes, Ecotoxicol. Environ. Saf., 202 (2020) 110924, doi: 10.1016/j.ecoenv.2020.110924.
[21] J. Pérez-Juste, I. Pastoriza-Santos, L.M. Liz-Marzán, Multi-functionality in metal@microgel colloidal nanocomposites, J. Mater. Chem. A, 1 (2013) 20–26.
[22] J.-H. Kim, B.W. Boote, J.A. Pham, J. Hu, H. Byun, Thermally tunable catalytic and optical properties of gold-hydrogel nanocomposites, Nanotechnology, 23 (2012) 275606, doi: 10.1088/0957-4484/23/27/275606.
[23] S. Wu, J. Dzubiella, J. Kaiser, M. Drechsler, X. Guo, M. Ballauff, Y. Lu, Thermosensitive Au-PNIPA yolk–shell nanoparticles with tunable selectivity for catalysis, Angew. Chem. Int. Ed., 51 (2012) 2229–2233.
[24] S. Shi, L. Zhang, T. Wang, Q. Wang, Y. Gao, N. Wang, Poly(N-isopropylacrylamide)–Au hybrid microgels: synthesis, characterization, thermally tunable optical and catalytic properties, Soft Matter, 9 (2013) 10966–10970.
[25] M. Ajmal, Z.H. Farooqi, M. Siddiq, Silver nanoparticles containing hybrid polymer microgels with tunable surface plasmon resonance and catalytic activity, Korean J. Chem. Eng., 30 (2013) 2030–2036.
[26] X.-J. Zhou, H.-P. Lu, L.-L. Kong, D. Zhang, W. Zhang, J.-J. Nie, J.-Y. Yuan, B.-Y. Du, X.-P. Wang, Thermo-sensitive microgels supported gold nanoparticles as temperature-mediated catalyst, Chin. J. Polym. Sci., 37 (2019) 235–242.
[27] M. Díaz, A. Barrera, S. López-Cuenca, S.Y. Martínez-Salazar, M. Rabelero, I. Ceja, V.V.A. Fernández, J. Aguilar, Size-controlled gold nanoparticles inside polyacrylamide microgels, J. Appl. Polym. Sci., 133 (2016) 43560, doi: 10.1002/app.43560.
[28] S.R. Khan, S. Ali, B. Ullah, S. Jamil, T. Zanib, Synthesis of iron nanoparticles in poly(N-isopropylacrylamide-acrylic acid) hybrid microgels for catalytic reduction of series of organic pollutants: a first approach, J. Nanopart. Res., 22 (2020) 1–12.
[29] X. Huang, M.A. El-Sayed, Gold nanoparticles: optical properties and implementations in cancer diagnosis and photothermal therapy, J. Adv. Res., 1 (2010) 13–28.
[30] T. Kamal, S.B. Khan, A.M. Asiri, Synthesis of zero-valent Cu nanoparticles in the chitosan coating layer on cellulose microfibers: evaluation of azo dyes catalytic reduction, Cellulose, 23 (2016) 1911–1923.
[31] L.A. Shah, A. Haleem, M. Sayed, M. Siddiq, Synthesis of sensitive hybrid polymer microgels for catalytic reduction of organic pollutants, J. Environ. Chem. Eng., 4 (2016) 3492–3497.
[32] C. Umamaheswari, A. Lakshmanan, N. Nagarajan, Green synthesis, characterization and catalytic degradation studies of gold nanoparticles against Congo red and Methyl orange, J. Photochem. Photobiol., B, 178 (2018) 33–39.
[33] B.R. Ganapuram, M. Alle, R. Dadigala, A. Dasari, V. Maragoni, V. Guttena, Catalytic reduction of methylene blue and Congo red dyes using green synthesized gold nanoparticles capped by *Salmalia malabarica* gum, Int. Nano Lett., 5 (2015) 215–222.
[34] N.Y. Nadaf, S.S. Kanase, Biosynthesis of gold nanoparticles by *Bacillus marisflavi* and its potential in catalytic dye degradation, Arabian J. Chem., 12 (2019) 4806–4814.